JACS
JOURNAL OF THE AMERICAN CHEMICAL SOCIETY
Communication
pubs.acs.org/JACS

Torsional Constraints of DNA Substrates Impact Cas9 Cleavage

Michael H. Räz,[§] Kumi Hidaka,[‡] Shana J. Sturla,[§] Hiroshi Sugiyama,*[,†,‡] and Masayuki Endo*[,†]

[†]Institute for Integrated Cell-Material Sciences (WPI-iCeMS), Kyoto University, Yoshida-ushinomiyacho, Sakyo-ku, Kyoto 606-8501, Japan

[‡]Department of Chemistry, Graduate School of Science, Kyoto University, Kitashirakawa-oiwakecho, Sakyo-ku, Kyoto 606-8502, Japan

[§]Department of Health Sciences and Technology, ETH Zürich, Schmelzbergstrasse 9, 8092 Zürich, Switzerland

Supporting Information

ABSTRACT: To examine the effect of the torsional constraints imposed on DNA substrates on Cas9 cleavage, we prepared constrained DNA substrates using a DNA origami frame. By fixing the dsDNA at the connectors of the DNA frame, we created torsionally constrained or relaxed substrates. We quantified the cleavage of constrained and relaxed substrates by Cas9 with qPCR. Moreover, we observed the Cas9/sgRNA complex bound to the DNA substrates and characterized the dissociation of the complex with high-speed atomic force microscopy. The results revealed that the constrained nontarget strand reduced the cleavage efficiency of Cas9 drastically, whereas torsional constraints on the target strand had little effect on the cleavage. The present study suggests that highly ordered and constrained DNA structures could be obstacles for Cas9 and additionally provides insights in Cas9 dissociation at a single molecule level.

In eukaryotic cells, DNA often has highly ordered structures and mechanical constraints such as molecular crowding, motor-driven activities, or chromatin remodeling, which can be topological barriers to protein interactions.[1] The Cas9 protein, derived from *Streptococcus pyogenes*, together with a single guide RNA (sgRNA) has evolved into a powerful tool for programmed genome editing.[2] Cas9 is an endonuclease associated with the prokaryotic adaptive immune system CRISPR (clustered regularly interspaced palindromic repeats). The sgRNA detects a complementary target sequence that contains a protospacer adjacent motif (PAM), and Cas9 subsequently cleaves the recognized DNA by using its HNH and RuvC nuclease domains (Figure 1A).[3] Current research is focused on increasing the specificity of Cas9 by understanding and optimizing interactions between the target sequence and the sgRNA.[4,5] However, the specificity of the sgRNA only partly predicts and explains the activity of Cas9.[4,5]

Cas9 is derived from archaea and bacteria[6] and therefore not well adapted to large eukaryotic genomes, which are arranged in chromosomes and tightly packed in nucleosomes. Recently it was reported that Cas9 binding and cleavage at nucleosomes are hindered[7] or rely on DNA breathing.[8] Furthermore, single-molecule studies demonstrated that euchromatin regions facilitate Cas9 binding, whereas the densely packed heterochromatin regions were not readily accessible.[9] These observations suggest that constrained DNA substrates might present an obstacle, limiting the activity and efficiency of Cas9 in eukaryotic cells, but the relationship between DNA constraints and DNA-Cas9 dynamics is not well understood.

Combining high-speed atomic force microscopy (AFM) with the spatial layout of DNA origami offers a powerful means to investigate DNA−protein interactions at a single-molecule level.[10] This approach was previously used to characterize the effect of tension-controlled dsDNA on DNA methylation and base excision repair[11,12] as well as DNA recombination.[13] In addition, the use of the DNA origami technique allows one to impose torsional constraints on DNA substrates by changing the connections of the sticky ends of the dsDNA to a DNA origami-based frame (DNA frame), designed to prevent torsional movement. This strategy was employed to suppress the B−Z transition (helical rotation) and consequently inhibit binding of a Z-DNA protein,[14] demonstrating the regulation of protein−DNA interaction by the torsional dynamics of dsDNA.

Herein, we used a DNA frame to visualize at a single-molecule level the binding of the Cas9 nuclease to four different DNA substrates with controllable torsional constraints (Figure 1B). We quantified the ability of Cas9 to cleave the torsionally constrained or rotatable dsDNA by quantitative PCR (qPCR) and followed the reaction by high-speed AFM. The DNA frame, rectangular, with a vacant inner area and connectors for the hybridization of a DNA substrate,[13] involves self-assembly of the M13mp18 ssDNA, staple strands, and the DNA substrate (Figure S1). The dsDNA substrates were prepared from four different ssDNA strands. Two 80-nucleotides (nt) strands [nontarget (NT80) and target (T80)] and two 96-nt strands [nontarget (NT96) and target (T96)] were used (Figure 1D). NT80 and NT96 contain the PAM sequence, and together with T80 and T96 they can form a 64 bp dsDNA template with two noncomplementary terminal regions for hybridization to the DNA frame. NT96 and T96 have two 16-bp terminal sequences for hybridization to both connectors, whereas NT80 and T80 are composed of only one 16-bp hybridization site allowing for the attachment to one or the other connector (Figure 1C,D). By combining NT96 and T96, both strands are attached to both connectors, which prevents torsional movement (substrate **I**). The combination of NT96 and T80 anchors the nontarget strand to both connectors, whereby only the target strand is allowed

Received: August 31, 2016
Published: October 6, 2016

DOI: 10.1021/jacs.6b08915
J. Am. Chem. Soc. 2016, 138, 13842−13845

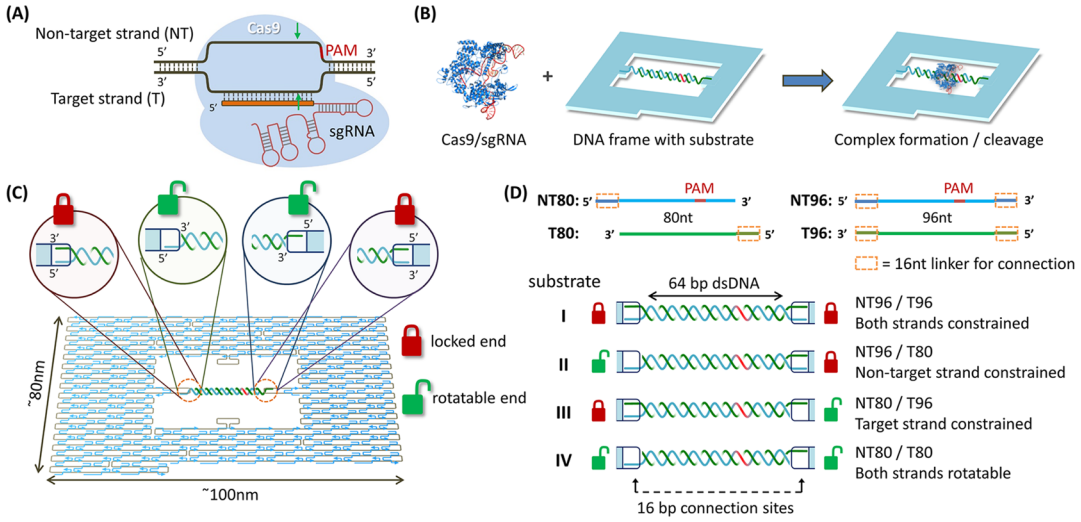

Figure 1. (A) Illustration of the Cas9 complex containing sgRNA and the dsDNA substrate (green arrows indicate cleavage sites). (B) DNA origami frame with substrate DNA strands was first prepared and then incubated with Cas9/sgRNA to examine the reaction. (C) The substrate strands were hybridized with the connectors inside the DNA origami frame. To prevent torsional movement, both strands were hybridized to the connectors (red, closed locks) or only one substrate strand was hybridized with the connector allowing the other to stay rotatable (green, open locks). (D) Representation of the four different substrates (**I**–**IV**).

torsional movement (substrate **II**). In contrast, hybridization of NT80 and T96 with the DNA frame keeps the nontarget strand constrained (substrate **III**), and combining NT80 and T80 results in an torsionally relaxed substrate with each strand attached to only one connector (substrate **IV**).

We examined the binding of Cas9 to substrates **I**–**IV** in the DNA frame. The reaction was performed in a buffer containing 10 mM Tris-HCl (pH 7.6), 10 mM NaCl, 10 mM $MgCl_2$, and 0.1 mM EDTA. We assembled substrate DNAs into the DNA frame using the same buffer and observed the substrate attachment by AFM (Figures 2A and S4–S7). The buffer was optimized to maintain the structural integrity of the DNA frame and simultaneously preserve the activity of Cas9, and its suitability was confirmed in a Cas9 digestion reaction of free substrate **IV** (Figure S3). To observe Cas9 binding, we preincubated equimolar amounts of Cas9 and sgRNA (10 nM) for 10 min at 25 °C and subsequently incubated it with 1 nM of the substrate DNA frames at 37 °C (Figure 1B). AFM images were obtained after 30 min with a substrate **IV** DNA frame (Figure 2B,C). It could be clearly visualized (Figure 2B, green arrows) and distinguished from the DNA frame on the basis of a bright spot at the center of the substrate, which was attributed as the Cas9 nuclease bound to the substrate (Figure 2B,C, blue arrows). We also detected DNA frames with an undefined structure, which appeared to be the cleaved DNA substrate, but we were unable to confirm whether it resulted from DNA cleaved by Cas9, Cas9 dissociation from the substrate or simply incorrectly annealed substrates within the DNA frame. Cas9 binding was investigated in more detail by an AFM-based time-course analysis for each of the substrates **I**–**IV**. The reactions were initiated as described earlier, and after 30, 90, 240, and 1200 min, micrographs were recorded (Figures S4–S7). We distinguished three different DNA frame situations: complexed, intact, and undefined (quantified data shown in Figure 2D–G). Substrates **III** and **IV** showed fast complex formation, and after 30 min, the complexed DNA frame exceeded the amount of intact frames and reached a peak of 55% after 90 min. Although complex formation for **I** and **II** was slower at the beginning, we observed a peak after 240 min, which reached also 55% complex formation.

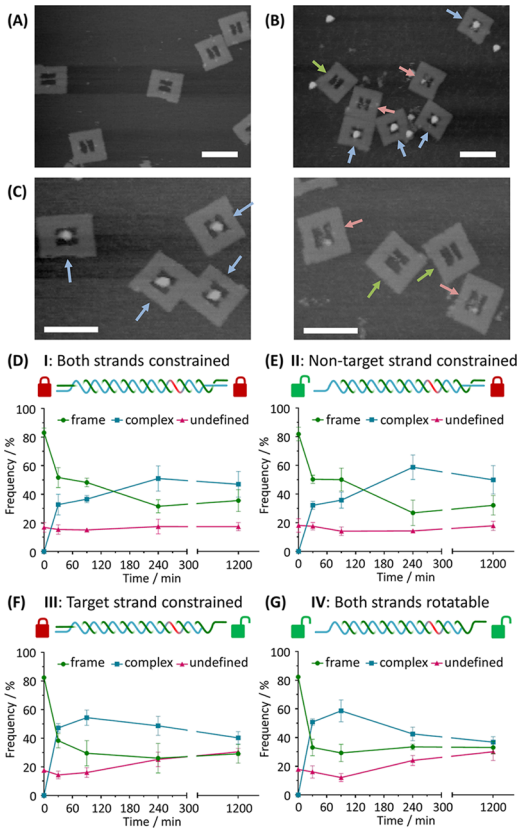

Figure 2. AFM imaging. (A) Substrate-containing DNA frame. (B) Complex of Cas9 with substrate **IV** in the DNA frame (blue arrow) was distinguished from the intact DNA frame (green arrow) and the undefined DNA frame (red arrow). (C) Magnification of intact, complexed, or undefined DNA frames. Scale bars 100 nm. (D–G) Time-course measurement for substrates **I**–**IV** (total of 300–400 DNA frames were analyzed for each time point). Error bars represent SD based on three individual experiments.

Noteworthy, for all four substrates we observed that 35% or more of the frames still had Cas9 bound to the substrate after 1200

DOI: 10.1021/jacs.6b08915
J. Am. Chem. Soc. 2016, 138, 13842–13845

min. These data confirm previous results, which suggested a long lifetime of the Cas9−DNA complex.[15] Moreover, the torsionally constrained nontarget strand seems to slow down complex formation, potentially due to slower DNA unwinding and recognition of the PAM sequence but it does not exclude binding of Cas9. Interestingly, for **III** and **IV**, the percentage of undefined DNA frames increased to 30% after 1200 min, whereas for **I** and **II**, the percentage of undefined DNA frames remained constant throughout the complete measurement. The increase of undefined DNA frames was mainly attributed to a decrease of complexed DNA frames, whereas the intact frames remained mainly unchanged. This result indicates that the constrained nontarget strand might have an effect on either the cleavage of the DNA substrate or the dissociation of Cas9 from the substrate, or both.

To confirm and quantify the cleavage reaction, we examined the effect of the torsionally constrained nontarget sequence by qPCR. If Cas9 is unable to cleave the substrates, the sequence is expected to be amplified, but if Cas9 cleaves the substrates, no or decreased PCR amplification of the target is expected (Figure 3A). To avoid background amplification from unhybridized

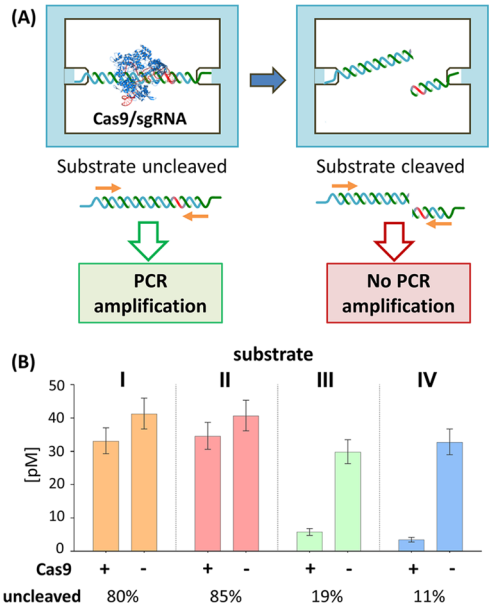

Figure 3. Quantification of the cleavage of substrates **I**−**IV** by Cas9. (A) Working hypothesis for qPCR analysis of the substrate cleavage by Cas9. (B) Estimation of the initial substrate concentration in the DNA frame for the Cas9+ or control reaction (Cas9−) after 60 min. Relative percentage of the uncleaved DNA substrate for each substrate compared to the reaction without Cas9− is indicated. The data were collected from at least five individual experiments for each substrate. Error bars represent the upper and lower limit of the 95% confidence interval.

substrate, we used the gel-purified substrate containing DNA frame and confirmed the intact DNA frame by AFM (Figures S8 and S9). To estimate the initial concentration and the cleavage of the hybridized substrate within the DNA frame, experiments were carried out using half of the sample for each frame recovered after gel purification (Cas9+), and the other half was used for a control reaction lacking Cas9 (Cas9−). For all four substrates, specific amplification was detected (Figure S10 and Table S5). For the control reactions (Cas9−), we quantified initial concentrations of ∼40 pM for **I** and **II** and ∼30 pM for **III** and **IV**. The Cas9 cleavage reactions (Cas9+) showed slightly decreased concentrations for **I** and **II** with ∼30 pM (Figure 3B and Table S3) and drastically decreased concentrations of only 3−5 pM for **III** and **IV**. We determined the ratios for the uncleaved fraction of the Cas9+ and Cas9− reactions. Only ∼20% of **I** and **II** were cleaved, whereas 81% of **III** and 89% of **IV** were cleaved. Although Cas9 can bind to the torsionally constrained substrates **I** and **II**, the nuclease seems unable to cleave them efficiently. Nevertheless, we were curious to test if additional substrate cleavage would be detected after 240 min. Cas9 cleavage reactions were carried out at 37 °C for up to 240 min and were subsequently analyzed by qPCR (Table S4). For **I** and **II**, only 20% of the substrate were cleaved after 240 min. In contrast, the cleaved fraction of **III** increased by 10%, to 90%, and **IV** remained unchanged with a cleaved fraction of 90% (Figure S11). This finding further supported our hypothesis that the constrained nontarget strand leads to reduced substrate cleavage. Previous studies reported that the Cas9/sgRNA complex first binds to the PAM sequence and subsequently opens the adjacent dsDNA.[16,17] The constrained dsDNA might therefore partially be opened at the PAM site, resulting in incomplete hybridization of the sgRNA, which would explain the observed binding of the Cas9/sgRNA complex to the constrained substrates.[16,17] The constrained dsDNA might therefore partially be opened at the PAM site, resulting in incomplete hybridization of the sgRNA, which would explain the observed binding of the Cas9/sgRNA complex to the constrained substrates. However, as described earlier, sufficient RNA−DNA complementarity between the sgRNA and the target DNA strand is needed to induce a conformational change in Cas9, which activates nuclease domains HNH and RuvC, which are responsible for cleavage of the dsDNA.[18] The constrained nontarget strands (**I** and **II**) seem to suppress complete hybridization of the sgRNA with the target strand and thereby cleavage is reduced, possibly by incomplete activation of HNH and RuvC. Cleavage of **III**, on the other hand, proceeds similar to the relaxed substrate **IV**. These results indicate that the relaxation of the nontarget strand is critical for initiation of Cas9 cleavage and seems to be important for full hybridization with the sgRNA.

Finally, we performed single-molecule AFM measurements of the presumed cleavage reaction of Cas9 from the DNA substrate (Figure 4, Figure S12). We observed the Cas9 nuclease bound to substrate **IV**-containing DNA frames. Time-lapse AFM scanning was performed for single frames with the bound complex (0.2 frames per second). The transition from Cas9 being clearly visible on the substrate, dissociating away from the DNA, and then completely disappearing from the frame occurred within approximately 30 s of observation. By following the reaction, it became apparent that the vacant area of the frame was occupied by the decomposed Cas9/sgRNA complex and the cleaved substrate. When Cas9 forms a complex with sgRNA and the target DNA, it is organized in an α-helical recognition lobe and a nuclease lobe. Both lobes undergo conformational rearrangement upon sgRNA binding and form a central channel to capture the target DNA.[19,20] The present AFM measurement suggests that the Cas9/sgRNA complex dissociates from the dsDNA by opening the lobes, whereby one of them seems to remain bound to the substrate (Figure 4A, 15−25 s). On the basis of height profiles of the Cas9/sgRNA−dsDNA complex, we observed a distinct reduction in the height from the active to the decomposed complex, which is still larger than the dsDNA in the frame, possibly accounted for by what may resemble the decomposed lobes of the complex (Figure 4B,C).

DOI: 10.1021/jacs.6b08915
J. Am. Chem. Soc. 2016, 138, 13842−13845

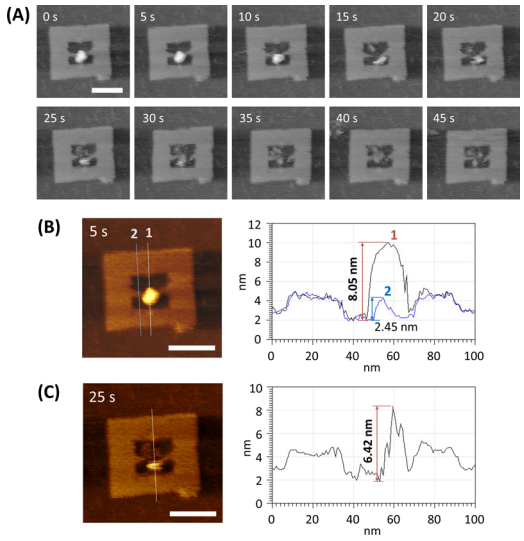

Figure 4. (A) Representative time-lapse AFM images of the dissociation of Cas9 from a single substrate **IV**-containing DNA frame. Height profile plot, taken from the Cas9/sgRNA–dsDNA complex at (B) 5 s and (C) 25 s. Numbers in the image correspond to the numbers in the height profile plot. Scale bar 50 nm.

By single-molecule approaches involving a DNA frame, we observed the constraint-dependent cleavage of DNA by Cas9. The spatial definition of the DNA by the DNA frame facilitated the dissection of the influences of torsional constraints of the target versus nontarget strand. We found that a constrained nontarget strand allows Cas9 to bind the target sequence; however, it drastically reduces the cleavage efficiency of the substrate. On the other hand, no significant decrease in the cleavage efficiency was observed when the target strand itself was constrained. The present study indicates that highly ordered DNA structures and constrained DNA could influence the activity of Cas9, potentially reducing its efficiency for certain genomic regions or chromatin states. In addition, observing the shape changes of the Cas9/sgRNA complex upon dissociation from the dsDNA provided insights into the enzyme mechanism at a single-molecule level. Finally, the versatility of the DNA frame suggests its general utility for investigating DNA–protein dynamics controlled by diverse physical properties of DNA strands.

■ ASSOCIATED CONTENT

Supporting Information

The Supporting Information is available free of charge on the ACS Publications website at DOI: 10.1021/jacs.6b08915.

Materials, experimental methods, AFM and qPCR data (PDF)

High-speed AFM movie (AVI)

High-speed AFM movie (AVI)

■ AUTHOR INFORMATION

Corresponding Authors

*endo@kuchem.kyoto-u.ac.jp

*hs@kuchem.kyoto-u.ac.jp

Notes

The authors declare no competing financial interest.

■ ACKNOWLEDGMENTS

We thank the Bilateral Japanese-Swiss Science and Technology Program between JSPS and ETH Zürich. This work was supported by JSPS KAKENHI (24104002, 15H03837, 16K14033) to M.E. and the Swiss National Science Foundation (156280) and the ETH research commission (ETH-43 14-1) to S.J.S. Financial support from The Novartis Foundation and The Naito Foundation to M.E. is acknowledged.

■ REFERENCES

(1) Milstein, J. N.; Meiners, J. C. *J. R. Soc., Interface* **2011**, *8*, 1673.
(2) Doudna, J. A.; Charpentier, E. *Science* **2014**, *346*, 1258096.
(3) Jinek, M.; Chylinski, K.; Fonfara, I.; Hauer, M.; Doudna, J. A.; Charpentier, E. *Science* **2012**, *337*, 816.
(4) Chari, R.; Mali, P.; Moosburner, M.; Church, G. M. *Nat. Methods* **2015**, *12*, 823.
(5) Xu, H.; Xiao, T.; Chen, C. H.; Li, W.; Meyer, C. A.; Wu, Q.; Wu, D.; Cong, L.; Zhang, F.; Liu, J. S.; Brown, M.; Liu, X. S. *Genome Res.* **2015**, *25*, 1147.
(6) Makarova, K. S.; Wolf, Y. I.; Alkhnbashi, O. S.; Costa, F.; Shah, S. A.; Saunders, S. J.; Barrangou, R.; Brouns, S. J.; Charpentier, E.; Haft, D. H.; Horvath, P.; Moineau, S.; Mojica, F. J.; Terns, R. M.; Terns, M. P.; White, M. F.; Yakunin, A. F.; Garrett, R. A.; van der Oost, J.; Backofen, R.; Koonin, E. V. *Nat. Rev. Microbiol.* **2015**, *13*, 722.
(7) Horlbeck, M. A.; Witkowsky, L. B.; Guglielmi, B.; Replogle, J. M.; Gilbert, L. A.; Villalta, J. E.; Torigoe, S. E.; Tjian, R.; Weissman, J. S. *eLife* **2016**, *5*, e12677.
(8) Isaac, R. S.; Jiang, F.; Doudna, J. A.; Lim, W. A.; Narlikar, G. J.; Almeida, R. *eLife* **2016**, *5*, e13450.
(9) Knight, S. C.; Xie, L.; Deng, W.; Guglielmi, B.; Witkowsky, L. B.; Bosanac, L.; Zhang, E. T.; El Beheiry, M.; Masson, J. B.; Dahan, M.; Liu, Z.; Doudna, J. A.; Tjian, R. *Science* **2015**, *350*, 823.
(10) Endo, M.; Sugiyama, H. *Acc. Chem. Res.* **2014**, *47*, 1645.
(11) Endo, M.; Katsuda, Y.; Hidaka, K.; Sugiyama, H. *J. Am. Chem. Soc.* **2010**, *132*, 1592.
(12) Endo, M.; Katsuda, Y.; Hidaka, K.; Sugiyama, H. *Angew. Chem., Int. Ed.* **2010**, *49*, 9412.
(13) Suzuki, Y.; Endo, M.; Katsuda, Y.; Ou, K.; Hidaka, K.; Sugiyama, H. *J. Am. Chem. Soc.* **2014**, *136*, 211.
(14) Endo, M.; Inoue, M.; Suzuki, Y.; Masui, C.; Morinaga, H.; Hidaka, K.; Sugiyama, H. *Chem. Eur. J.* **2013**, *19*, 16887.
(15) Richardson, C. D.; Ray, G. J.; DeWitt, M. A.; Curie, G. L.; Corn, J. E. *Nat. Biotechnol.* **2016**, *34*, 339.
(16) Sternberg, S. H.; Redding, S.; Jinek, M.; Greene, E. C.; Doudna, J. A. *Nature* **2014**, *507*, 62.
(17) Wu, X.; Scott, D. A.; Kriz, A. J.; Chiu, A. C.; Hsu, P. D.; Dadon, D. B.; Cheng, A. W.; Trevino, A. E.; Konermann, S.; Chen, S.; Jaenisch, R.; Zhang, F.; Sharp, P. A. *Nat. Biotechnol.* **2014**, *32*, 670.
(18) Sternberg, S. H.; LaFrance, B.; Kaplan, M.; Doudna, J. A. *Nature* **2015**, *527*, 110.
(19) Jinek, M.; Jiang, F.; Taylor, D. W.; Sternberg, S. H.; Kaya, E.; Ma, E.; Anders, C.; Hauer, M.; Zhou, K.; Lin, S.; Kaplan, M.; Iavarone, A. T.; Charpentier, E.; Nogales, E.; Doudna, J. A. *Science* **2014**, *343*, 1247997.
(20) Nishimasu, H.; Ran, F. A.; Hsu, P. D.; Konermann, S.; Shehata, S. I.; Dohmae, N.; Ishitani, R.; Zhang, F.; Nureki, O. *Cell* **2014**, *156*, 935.

DOI: 10.1021/jacs.6b08915
J. Am. Chem. Soc. 2016, 138, 13842–13845